J. Fluid Mech. (1972), *vol.* 54, *part* 4, *pp.* 679–690
Printed in Great Britain

Semi-infinite vortex trails, and their relation to oscillating airfoils

By D. WEIHS
Department of Applied Mathematics and Theoretical Physics, University of Cambridge

(Received 4 May 1972)

Semi-infinite double rows of vortices are used to study the periodic wake of both oscillating and stationary two-dimensional bodies immersed in a uniform incompressible stream. Analytical expressions for the induced velocities on the body, for trails with constant spacing, which are valid for small values of the oscillation amplitude are presented while, for the general case of vortex shedding, an iterative procedure for the representation of trails of variable spacing is developed and used. Vortex streets due to oscillating bodies are obtained as a function of three non-dimensional parameters: the Strouhal number (initial spacing ratio), a non-dimensional vortex strength and the downstream spacing ratio. Criteria establishing when such trails are expected to widen, become narrow or stay of constant width are presented, as well as expressions for the induced velocities.

The trails and their induced velocities enable the calculation of the vortex strength from measurable quantities. Thus they can serve as a method for estimating the hydrodynamic forces on the airfoil due to large amplitude oscillations, such as those observed in the propulsive movements of fish and cetaceans, as well as the small amplitude oscillations due to hydroelastic interactions.

1. Introduction

Most existing unsteady potential aerodynamic wing theory is based upon the assumption of small perturbations, with the subsequent linearization of the equations of motion. In these models (Robinson & Laurmann 1956) the vorticity shed from the moving airfoil is assumed to stay in the form of a plane sheet of velocity discontinuity trailing back from the instantaneous position of the airfoil trailing edge. This last assumption has long been known to be inaccurate (Rosenhead 1931), and experimental studies of oscillating airfoils (Bratt 1953; Clauss 1968; Wood & Kirmani 1970) have shown that the vortex sheet produced in many cases rolls up into two rather regular rows of alternating discrete vortices of opposite sign for wide ranges of frequencies and Reynolds numbers. Some of the more recent advanced nonlinear potential flow studies (Giesing 1968; Djojodihardjo & Widnall 1969) include these rolling-up effects. These are numerical works and are mainly designed for transient effects. An understanding of the wake flow pattern of an oscillating body is important as a method of obtaining the instantaneous circulation on the body and as a check on the assumption of

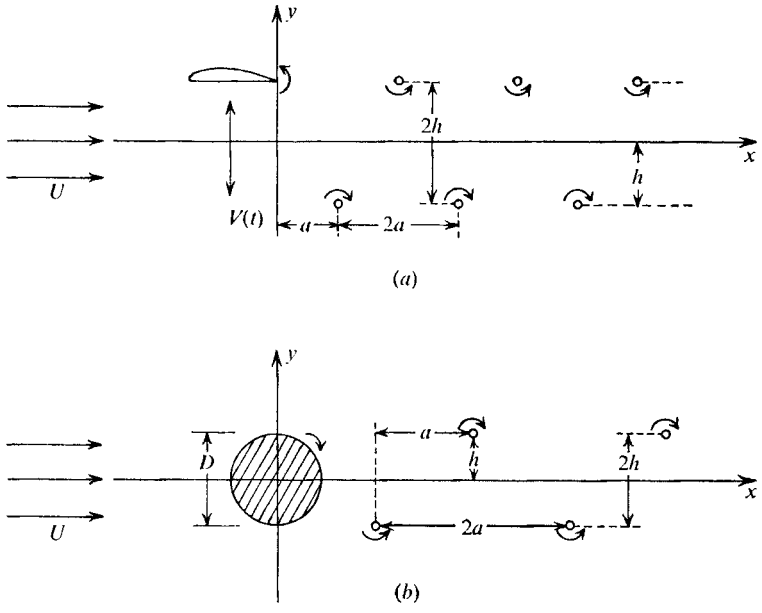

FIGURE 1. Schematic representation of vortex trails shed behind (*a*) an oscillating airfoil and (*b*) a bluff stationary body in a uniform incompressible inviscid stream.

classical theoretical calculations, in work on flutter, and in the analysis of oscillating vane propulsive systems, such as are used by many types of fish.

Vortex trails observed behind oscillating vanes with sharp trailing edges are reminiscent of the staggered Kármán vortex street (Milne-Thomson 1968; Lamb 1945), except for two characteristics (see figure 1).

(i) The sense of each vortex in the trail is opposite to that of the Kármán 'natural' shedding case.

(ii) Unlike the theoretical infinite street, the trail is at most of semi-infinite length, being shed from a certain region of the flow field.

The vortex trails shed from such oscillating foils will be designated as 'thrust-type' trails as the induced momentum produces thrust upon the disturbing body initiating the trail, while the vortex streets shed from stationary bodies produce drag, and will be called 'drag-type' (see figure 1). Trails of the latter type are also produced by oscillating blunt-based airfoils (Wood 1971). Theoretical studies of the Kármán vortex street have almost all been based upon the assumption of the existence of rows of infinite length, with the single exception of Synge (1926), who used semi-infinite rows to obtain the drag force on a cylinder. All these analyses have assumed trails of constant spacing, which implies that the vertical induced velocity on each vortex is zero. This is not correct for the vortices closest to the front end of the row, which actually have the largest influence upon the exciting body. As a result, the spacing of vortices in the trail varies as one moves along the trail away from the initial disturbance.

In the present work, some properties of semi-infinite double vortex trails with variable spacing in an inviscid fluid are studied, with possible implications for the circulation and forces induced on the vanes producing the streets. It is shown that

only for small values of the final spacing ratio does the assumption of constant spacing lead to a good approximation of the induced velocities.

Comparison of the results of present theory with experimental results shows good qualitative agreement for the shape of the ensuing trails. More quantitative comparison was hampered by lack of data on certain parameters, but the present results are shown to fall within the range of experimentally measured data.

2. Method of analysis

Consider first a semi-infinite single row of vortices each of strength k, located at the points $(2na, 0)$, where, $n = 0, 1, 2, \ldots, \infty$, in the x, y plane. The complex potential of this array is

$$\Omega = ik[\ln z + \ln(z-2a) + \ldots + \ln(z-2na) + \ldots]. \tag{1}$$

The complex conjugate velocity induced on the leading vortex (at $z = 0$) is

$$w = -\frac{\partial}{\partial z}(\Omega - ik\ln z)_{z=0} = -ik\sum_{n=1}^{\infty}\frac{1}{2na}, \tag{2}$$

which is not bounded, as the harmonic series diverges. As a result, such a row could not exist by itself, as each member would be displaced very rapidly upon its formation, not permitting the establishment of the row. In contrast, in an infinite row (Milne-Thomson 1968) there is no induced velocity on any of the vortices, as the remaining vortices may be grouped into equidistant pairs with cancelling induced velocities. For this case the complex potential can be expressed as an infinite product of the type

$$\Omega_1 = ik\ln\left[\frac{\pi z}{a}\prod_{n=1}^{\infty}\left(1-\frac{z^2}{4n^2a^2}\right)\right] = ik\ln\sin\frac{\pi z}{2a}. \tag{3}$$

Taking now two rows of vortices of semi-infinite length, with vorticity of opposite sign, the most realistic case is that of alternating vortex position, i.e. each vortex of the upper row is situated opposite the centre of the distance between the two closest vortices of the lower row (see figure 1).

The complex potential for this configuration is

$$\Omega = \pm ik\sum_{n=1}^{\infty}\ln(z-2na-ih) \mp ik\sum_{n=1}^{\infty}\ln(z-(2n-1)a+ih), \tag{4}$$

where the upper signs describe the trail shed by an oscillating airfoil and the lower signs give the trail shed by a stationary bluff object; $2a$ and $2h$ are the horizontal and vertical spacings, respectively.

The induced (conjugate) velocity at the point z is

$$w = \mp ik\sum_{n=1}^{\infty}\left(\frac{1}{z-2na-ih} - \frac{1}{z-(2n-1)a+ih}\right). \tag{5}$$

Omitting the self-induced velocities, (5) describes an alternating series, for which the Leibniz test establishes conditional convergence. One of the properties of such series is that the value of the sum of an arbitrarily large number of terms

depends upon the order of summation. This fact causes no difficulty here, as the physical case described (vortex shedding from an obstacle in a uniform stream) defines the order of summation, which is according to the distance of each vortex from the origin.

Equation (5) can be rewritten as

$$w = \mp ik \sum_{n=0}^{\infty} \left(\frac{1}{z-(2n+2)a-ih} - \frac{1}{z-(2n+1)a+ih} \right)$$
$$= \mp \frac{ik}{2a} \sum_{n=0}^{\infty} \left(\frac{1}{n-(z+ih-a)/2a} - \frac{1}{n-(z-ih-2a)/2a} \right). \tag{6}$$

However, from Gradshteyn & Ryshik (1965, p. 944) we have

$$\psi(x) - \psi(y) = \sum_{n=0}^{\infty} \left(\frac{1}{n+y} - \frac{1}{n+x} \right), \tag{7}$$

where
$$\psi(z) \equiv \frac{d}{dz}[\ln \Gamma(z)] = \int_0^{\infty} \left[e^{-t} - \frac{1}{(1+t)^z} \right] \frac{dt}{t}, \tag{8}$$

so that
$$u - iv = \mp \frac{ik}{2a} \left[\psi\left(-\frac{z-ih-2a}{2a} \right) - \psi\left(-\frac{z+ih-a}{2a} \right) \right], \tag{9}$$

where u, v are the x, y components of the induced velocity, and tabulated values of ψ appear in Abramowitz & Stegun (1965).

By applying (9) to the next vortex to be shed (at $z = 0+ih$, say), one sees that it will be displaced both horizontally and vertically. On the other hand, a vortex far down the line is in a situation approaching that of an infinite double row, so that the vertical velocities on it vanish and the horizontal induced velocity is close to

$$U_K = \pm \frac{k\pi}{2a} \tanh \frac{\pi h}{a}, \tag{10}$$

where U_K is the velocity of advance of the infinite Kármán trail (Milne-Thomson 1968) and the signs stand for the same cases as in (4).

From such considerations, one sees that semi-infinite double vortex rows will in general not have constant spacing. As a result, (9) can serve only as a first trial in a scheme of successive approximations. Nevertheless, it is extremely useful for obtaining a qualitative understanding of the behaviour of such trails and for defining parameters influencing this behaviour (see § 3).

More accurate expressions for the potential and induced velocity can be obtained by the following iterative process. Initially a trail with constant spacing is taken and the perturbations in position calculated from

$$x_n^{(j)} = x_{n-1}^{(j)} + \int_0^{\frac{1}{2}T} u_{n-1}^{(j)}\, dt + \tfrac{1}{2}UT, \tag{11a}$$

$$y_n^{(j)} = -y_{n-1}^{(j)} + \int_0^{\frac{1}{2}T} v_{n-1}^{(j)}\, dt, \tag{11b}$$

where j is the index number of the iteration, T is the shedding period and $x_n^{(0)}$, $y_n^{(0)}$, $u_n^{(0)}$ and $v_n^{(0)}$ are those appearing in (4)–(9). Having now found the positions of each of the vortices for the first iteration, the leading vortex is returned artificially

to the position $(0, h)$ and the new positions $x_n^{(2)}$ and $y_n^{(2)}$ calculated again from (11), where now the velocities $u_{n-1}^{(2)}$ and $v_{n-1}^{(2)}$ are obtained from

$$w_n^{(j)} = \mp ik \sum_{r=1}^{\infty} \left(\frac{1}{z_n^{(j)} - z_{2r-1}^{(j-1)}} - \frac{1}{z_n^{(j)} - z_{2r}^{(j-1)}} \right) \quad (2r, 2r-1 \neq n) \tag{12}$$

by substituting $j = 2$. The induced velocities are not explicit functions of the time t but of the instantaneous position, so that, to evaluate the integrals in (11), we employ the approximation

$$\int_0^{\frac{1}{2}T} u_n^{(j)}\, dt \simeq \sum_{p=0}^{m} u_{n,p}^{(j)} \frac{T}{2m}, \quad \int_0^{\frac{1}{2}T} v_n^{(j)}\, dt \simeq \sum_{p=0}^{m} v_{n,p}^{(j)} \frac{T}{2m}, \tag{13}$$

breaking the trajectory of each vortex during the half cycle into m sections of equal duration for which the induced velocity is assumed constant. These velocities are obtained from

$$w_{n,p}^{(j)} = \mp ik \sum_{n=1}^{\infty} \left(\frac{1}{z_{n,p}^{(j)} - z_{2r-1}^{(j-1)}} - \frac{1}{z_{n,p}^{(j)} - z_{2r}^{(j-1)}} \right). \tag{14}$$

The displacement of vortex n during each of the time steps p is given by

$$x_{n,p}^{(j)} = x_{n,p-1}^{(j)} + \frac{T}{2m}(u_{n,p-1}^{(j)} + U), \quad y_{n,p}^{(j)} = y_{n,p-1}^{(j)} + \frac{T}{2m} v_{n,p-1}^{(j)} \quad (p = 1, 2, \ldots, m), \tag{15}$$

and from (11)

$$x_{n,0}^{(j)} = x_{n-1}^{(j)} + \tfrac{1}{2}UT, \quad y_{n,0}^{(j)} = -y_{n-1}^{(j)}. \tag{16}$$

The perturbations in position from the initial 'constant spacing' trail were calculated using (11)–(16). This was continued till $n = 20$ or the perturbation was less than 0·5 % of the final spacing, whichever happened first. In the former case a nonlinear Shanks transformation was applied (Shanks 1955) to the alternating series obtained from the vertical position of the 20 vortices calculated, to get the final vertical position. The positions of the vortices were then taken as the basis of the next iteration. The number m of steps in (13) and the following analysis is arbitrary. The final positions of individual vortices were taken as fulfilling the condition

$$\left| \frac{u_n^{(j)} - u_n^{(j-1)}}{u_n^{(j)}} \right| \leqslant \epsilon, \quad \left| \frac{v_n^{(j)} - v_n^{(j-1)}}{v_n^{(j)}} \right| \leqslant \epsilon, \tag{17}$$

where ϵ is arbitrarily small (taken as 0·005 in the present calculations). The relative differences between final positions obtained when $m = 5$ and $m = 10$ were never larger than 1 % for the cases checked ($h/a \leqslant 1$).

The initial horizontal and vertical spacings are defined as $2d$ and $2b$, while the final (far from the vortex-producing disturbance) values are $2h$ and $2a$ respectively.

In the case of a cylinder of diameter D shedding a vortex trail

$$2d = UT, \quad 2b = D \quad \text{(approximately)} \tag{18}$$

and

$$S = D/UT \simeq b/d, \tag{19}$$

where U is the free-stream velocity. For an oscillating airfoil b is the distance from the point of shedding to the oscillation centre-line, and (19) is no longer an approximation.

3. Results and discussion

3.1. *Trails with constant spacing*

It has been shown in § 2 that this type of semi-infinite trail is not likely to be obtained from natural shedding situations, but it still has value as a first approximation. It should be as least as good a description of the flow field as the Kármán infinite trail, which also is of constant spacing. For such trails the induced velocity components are given by (9). In this case, the spacings are a and h respectively. The velocity induced on the curve

$$y = A\cos(\pi x/a) \quad (-\tfrac{1}{2}a \leqslant x \leqslant \tfrac{1}{2}a) \tag{20}$$

is the velocity induced on an oscillating foil during one-half of its cycle, assuming now that the airfoil may be represented by a concentrated vortex (the 'bound' vortex). The velocity induced during the other half of the cycle is obtained by use of the symmetry properties of the double row, the only difference being a change of sign in the v (the vertical component). Hence, calculation of the induced velocity on the half-cycle described by (20) is sufficient to obtain a mapping of induced velocities on the bound vortex at any time. These velocities are important, as they contribute to the circulation around the airfoil, i.e. the strength of the bound vortex.

When looking at periodic vortex shedding from a stationary body with separated flow, the induced velocity is the cause of the net circulation around the body, causing the asymmetric shedding. From now on, the discussion will be for oscillating airfoils, unless specifically mentioned otherwise.

The point $(0, h)$ is especially interesting as this is the point of appearance of the next vortex. Leaving out the possible physical mechanism producing the vortex trail for the moment, the velocity induced on this vortex leads to an understanding of the possible distortions of the trail.

For this point, the infinite sums in (4) and (5) are simplified, giving

$$u_{(0,h)} = \frac{k}{a}\sum_{n=1}^{\infty}\left(\frac{2h/a}{(2n-1)^2+(2h/a)^2}\right), \tag{21a}$$

$$v_{(0,h)} = \frac{k}{a}\sum_{n=1}^{\infty}\left(\frac{2n-1}{(2n-1)^2+(2h/a)^2}-\frac{1}{2n}\right). \tag{21b}$$

The horizontal velocity component is, by symmetry considerations of the infinite Kármán trail,

$$u_{(0,h)} = \tfrac{1}{2}U_K = \tfrac{1}{4}\pi(k/a)\tanh(\pi h/a). \tag{22}$$

The vertical component is more complicated, and after some manipulation can be written as

$$\begin{aligned} v_{(0,h)} &= \frac{k}{a}\sum_{n=1}^{\infty}\left(\frac{1}{2n-1}-\frac{1}{2n}-\frac{(2h/a)^2}{(2n-1)[(2n-1)^2+(2h/a)^2]}\right) \\ &= \frac{k}{a}\Bigg[\ln 2+\sum_{j=1}^{N}\sum_{n=1}^{\infty}(-1)^j\frac{(2h/a)^{2j}}{(2n-1)^{2j+1}} \\ &\quad +(-1)^N\sum_{n=1}^{\infty}\frac{(2h/a)^{2N+2}}{(2n-1)^{2N+1}[(2n-1)^2+(2h/a)^2]}\Bigg], \end{aligned} \tag{23}$$

and the value of the first summation term can be represented by Riemann zeta functions. When $h/a \to 0$, which for finite free-stream velocity and oscillation frequency means vanishing amplitude, (22) and (23) give

$$u = 0, \quad v = (k/a)\ln 2 = (kf/U)\,2\ln 2. \tag{24}$$

The usual assumption for the small amplitude harmonic oscillation of an airfoil in unsteady aerodynamic theory is that each element of the wake stays exactly where it was shed, relative to the undisturbed flow (Robinson & Laurmann 1956). From (24), we see that this assumption is correct only for the horizontal (streamwise) component. The vertical-induced velocity tends to a value proportional to the circulation, and the oscillation (shedding) frequency f, and inversely proportional to the free-stream velocity. This component causes the widening of initially very narrow trails and affects the circulation on the bound vortex by inducing an additional angle of incidence. It is useful to non-dimensionalize the velocity components by the following definitions:

$$u' \equiv ua/k, \quad v' = va/k. \tag{25}$$

Using these definitions in conjunction with (22) and (23), the effect of changing the spacing ratio h/a is now examined. For $h/a \ll 1$, which is of interest in aeroelastic studies,

$$u'_{(0,h)} \simeq \tfrac{1}{4}\pi^2 h/a \tag{26}$$

and

$$v'_{(0,h)} \simeq \ln 2 - \left(\frac{2h}{a}\right)^2 \sum_{n=1}^{\infty} \frac{1}{(2n-1)^3} + \left(\frac{2h}{a}\right)^4 \sum_{n=1}^{\infty} \frac{1}{(2n-1)^5} - O\left(\frac{h}{a}\right)^6$$

or

$$v'_{(0,h)} \simeq \ln 2 - \frac{7}{2}\left(\frac{h}{a}\right)^2 \zeta_{(3)} + O\left(\frac{h}{a}\right)^4 \zeta_{(5)}, \tag{27}$$

where ζ is the Riemann zeta function. The formulation of (23) was required to obtain the vertical component of velocity as a function of ascending powers of the spacing ratio and tabulated functions. This approach is rapidly convergent for $2h/a < 1$. For general h/a it is simpler to calculate the velocity directly from (9), which, however, is not explicitly dependent upon the spacing ratio, while the form of (27) is more useful for the small values of h/a encountered in practice (Wood & Kirmani 1970; Bratt 1953; also see figure 2 of this paper).

From (27) we see that $v'_{(0,h)}$ drops by only 1 % when $0 < h/a < 0{\cdot}04$. This leads to a concept of a 'linear' range of spacing ratios in which the vertical component is approximately constant, while the horizontal component increases linearly with the spacing ratio. In this range, the results are approximately valid for trails with variable spacing too. Increasing the value of h/a causes a monotonic increase in $u'_{(0,h)}$ and a decrease in $v'_{(0,h)}$ (see figure 2), which for a certain value of h/a becomes negative. Trial-and-error calculations have determined this value as $h/a = 0{\cdot}637$ to three-figure accuracy, which to the same accuracy is equal to $2/\pi$. No special significance is attached to this fact, which may be a hint to some as yet unnoticed relationship. A further increase in h/a causes a sharp continuing decrease in the signed value of $v'_{(0,h)}$ while $u'_{(0,h)}$ tends to the value $\frac{1}{4}\pi k/a$ (from equation (22)). The main conclusion to be drawn from this dependence upon the

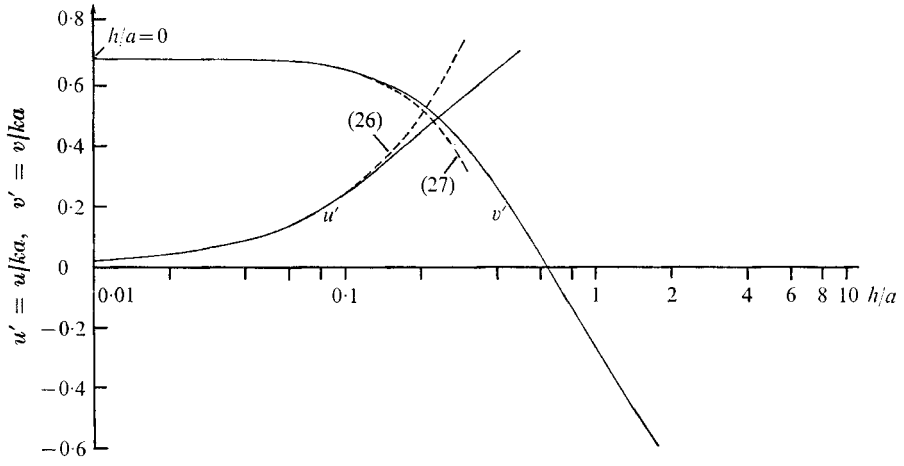

FIGURE 2. Horizontal and vertical non-dimensional induced velocities on the leading vortex as a function of the spacing ratio, for trails with constant spacing. The broken lines show the approximate solution for small h/a.

ratio h/a is that, for trails with variable spacing ratios, when the initial ratio is less than a certain (as yet unknown) value, the vertical spacing will tend to increase, while for larger ratios, it will decrease. The streamwise spacing on the other hand always increases owing to the velocities induced by the trail. Also, when the spacing ratio increases, the feedback effect of the wake on the bound circulation (and the forces) decreases rapidly, after an initial small range in which it is almost constant. This results from the relationship between the induced angle of incidence and the induced velocities:

$$\alpha_i = \arctan[v/(U+u)]. \tag{28}$$

Next, a rather crude approximation was employed to obtain a better idea of the transition from widening to narrowing vortex streets. Here it was assumed that one vortex only was free to move, according to the induced velocity upon it, the others being constrained to stay in the regular street with constant spacing. Not surprisingly, the results of this calculation showed that when $h/a \simeq 0{\cdot}288$ the movable vortex returned to its place in the trail, while it moved outwards for smaller ratios and inwards for larger ratios. This analysis is similar to the Kármán stability analysis, which shows that for $h/a \simeq 0{\cdot}281$ initial displacements of vortices are damped out to the first order, so that the small difference in the 'critical' value of the spacing ratio is probably due to a combination of computational errors, and the slightly different approach.

3.2. *Trails with variable spacing*

The velocities induced on the individual vortices cause the vertical and horizontal spacings to change from the ones set by the amplitude and frequency of oscillation of the airfoil and the free-stream velocity. These changes in shape of the vortex trail depend on all the factors mentioned as well as the magnitude of the vorticity, so that general analytical expressions describing the form of the trail would be extremely complicated. Even numerical calculations are difficult

because of the infinite number of vortices, the feedback effect of the positioning of these vortices upon the strength, and the implicit relations between the induced velocities and time.

Define the differences between the final (far from the flow disturbance, when the vortex trail has become of constant spacing) and initial spacings as

$$\Delta x = a - d, \quad \Delta y = h - b. \tag{29}$$

Under the same assumption that the trail finally reaches a state of constant spacing, the induced velocity will approach the value obtained from classical infinite double vortex rows, so that

$$a = d + \tfrac{1}{2} U_K T \tag{30}$$

and from (18)

$$a = \tfrac{1}{2} UT(1 + U_K/U), \tag{31}$$

so, from (10),

$$a = \frac{UT}{2}\left(1 + \frac{1}{a}\frac{k}{U}\frac{\pi}{2}\tanh\frac{\pi h}{a}\right) \tag{32}$$

and

$$a = \tfrac{1}{4} UT[1 \pm (1 + \lambda(\sigma, h/a))^{\frac{1}{2}}]. \tag{33}$$

where $\lambda = 4\pi\sigma \tanh(\pi h/a)$ and $\sigma = k/U^2T$. But the spacing has to be non-negative, so that only the first solution is of interest, as λ is non-negative:

$$a = \tfrac{1}{4} UT[1 + (1 + \lambda)^{\frac{1}{2}}]. \tag{34}$$

For thrust-type vortex streets therefore, the horizontal spacing far from the initial disturbance is always larger than the initial spacing. From (29)

$$\frac{h}{a} = \frac{b + \Delta y}{\tfrac{1}{4} UT[1 + (1 + \lambda)^{\frac{1}{2}}]} \tag{35}$$

or

$$\frac{\Delta y}{b} = \frac{1}{S}\frac{h}{a}\frac{1 + (1 + \lambda)^{\frac{1}{2}}}{2} - 1, \tag{36}$$

from which the change in vertical distance between the rows, from the initial shedding distance, can be found. The most interesting question arising here is when is this change positive, and when negative. Trails of equal initial and final spacing are those for which $\Delta y = 0$ in (36), i.e.

$$S = \tfrac{1}{2}(h/a)[1 + (1 + \lambda)^{\frac{1}{2}}], \tag{37}$$

or by using the fact that $h = b$ in this case, (33) is retrieved. Thus, for each value of σ and h/a, a trail with $b = h$ (which does not mean constant spacing) can be found. These values lie on a curved surface whose projection on the S, h/a plane is shown in figure 3. This surface exists only in the first octant. Points below (to the right) the surface describe vertically widening trails, while points above the surface stand for contracting trails (see also figures 4 and 5).

The practical significance of expressions like (33) and (36) lies in the possibility of determining the vortex strength by means of measurable quantities such as the initial and final spacings of the vortices, the frequency and the free-stream velocity. This in turn would lead to an estimate for the upper bound of the circulation around the body. In actual vortex street shedding situations this has been

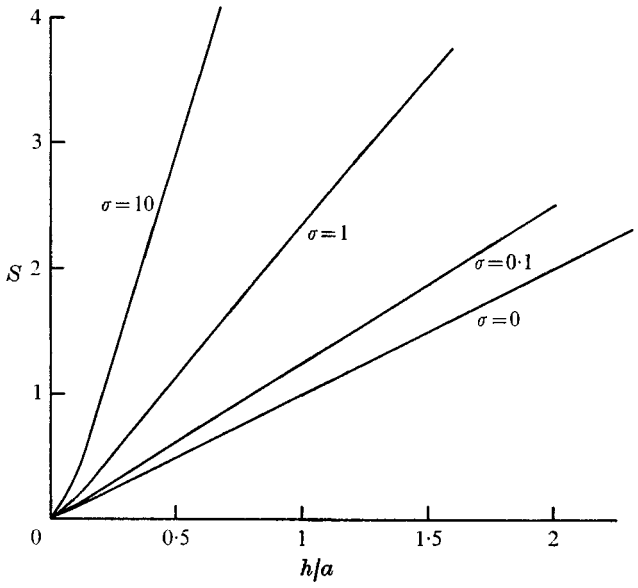

FIGURE 3. The Strouhal number (initial spacing ratio) as a function of the final spacing ratio for trails with equal initial and final vertical spacings. For each value of σ, points to the right of the relevant curve represent widening trails, while points to the left describe trails which become narrower.

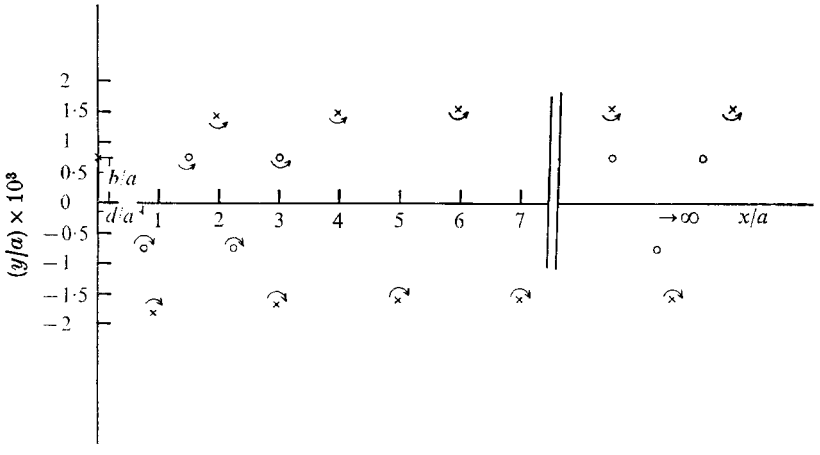

FIGURE 4. Vortex trail with $S = 10^{-3}$, $\sigma = k/U^2T = 1$. ×, position of vortex in actual trail; ○, position of vortex in constant-spacing trail with initial values of the horizontal and vertical spacings.

shown (Wood & Kirmani 1970) to be up to 50% higher than the circulation predicted by 'classical' unsteady airfoil theory. Existing experimental data (see § 1) do not include all the information required for such calculations (specifically the initial vertical spacing is missing), so that a full comparison cannot be made at present. Taking Wood & Kirmani's results, the circulation was calculated by (36) and was found to agree with their values of the circulation (which they obtained by integrating tangential velocity components) for instants of separation lagging by 20–50° behind the instant of maximum amplitude. In comparison,

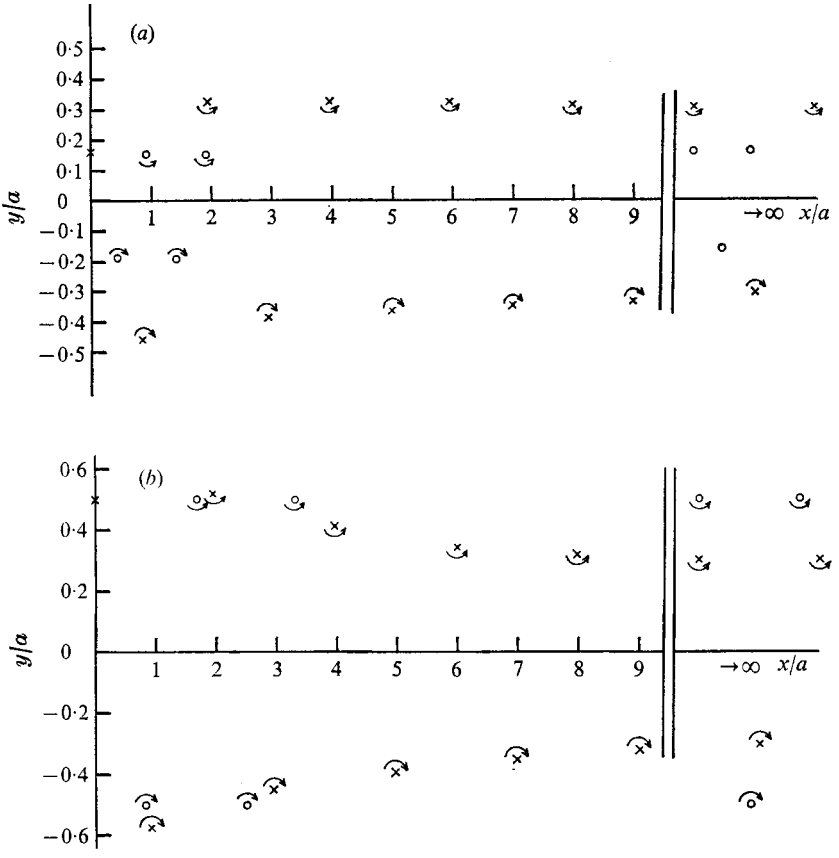

FIGURE 5. (*a*) Widening thrust-type trail with $S = 0{\cdot}335$, $\sigma = 1$ ($h/a \simeq 0{\cdot}305$). (*b*) Narrowing thrust-type trail with $S = 0{\cdot}6$, $\sigma = 0{\cdot}1$ ($h/a \simeq 0{\cdot}302$). See figure 4 for definition of symbols.

the aforementioned authors mention measuring separation points at 18–108° after the displacement peak.

Finally, computations of the actual shape of some thrust-type vortex trails, by use of (11)–(16), are shown in figures 4 and 5. The horizontal spacing increases very rapidly to its final value, the induced velocity reaching within 5 % of its final value at about $n = 6$ while the vertical spacing oscillates around the final value, approaching it rather slowly, being a harmonic series. Still, the final distance between rows in the trial may be obtained accurately from rather few vortex positions by means of the Shanks transformation mentioned before. This may be useful for future interpretation of experimental results by the methods presented here, as the usual experimentally observed vortex trail can be observed for relatively short distances behind the body. The trails in figures 4 and 5 all become wider initially, narrowing again at some distance from the airfoil towards the final regular pattern. Such behaviour is clearly seen in Bratt's (1953) smoke visualization of the wake of an oscillating airfoil.

The asymmetry in figures 4 and 5 is due to the fact that these are 'snapshots' of the trail at a certain time. Looking at the same trails one-half cycle later would

result in a mirror image of each figure reflected in the x/a axis (but with unchanged signs of vorticity).

4. Conclusion

The description of the wake of an oscillating vane by a semi-infinite double row of inviscid vortices presented here is suggested as a step towards a method of predicting the hydrodynamic forces on an airfoil performing finite amplitude oscillations, in an inviscid incompressible flow. This can be described formally as the approximation of the integral equation describing the mutual influence between the airfoil and the wake by an infinite series.

The semi-infinite trail used here is much more realistic than the usual assumption of infinite length, leading to changes in both vertical and horizontal spacing of the vortices as one advances down the street. The influence of these differences appears mainly in the velocities induced upon the exciting vane, for, far downstream the wake approaches the condition described by an infinite trail. The mean thrust (or drag) can therefore be calculated by Kármán's equations for the force (Milne-Thomson 1968) and the feedback effect on the vane appears in the vortex strength, and spacing ratio. Such results would be applicable to the analysis of the propulsive forces produced by scombroid fish and cetaceans who are propelled by large amplitude pitching and heaving oscillations of a 'lunate' tail fin of high aspect ratio.

The author wishes to thank Professor Sir James Lighthill for useful discussion and comments.

REFERENCES

ABRAMOWITZ, M. & STEGUN, I. A. 1965 *Handbook of Mathematical Functions*, chap. 6. Washington: National Bureau of Standards.

BRATT, J. B. 1953 *Aero. Res. Counc. R. & M.* no. 2773.

CLAUSS, G. 1968 *Z. ver. dtsch. Ing.* no. 1144.

DJOJODIHARDJO, R. H. & WIDNALL, S. E. 1969 *A.I.A.A. J.* **7**, 2001.

GIESING, J. P. 1968 *J. Aircraft*, **5**, 135.

GRADSHTEYN, I. S. & RYSHIK, I. M. 1965 *Tables of Integrals, Series and Products*, p. 944. Academic.

LAMB, H. 1945 *Hydrodynamics*, 6th edn., chap. 7. Dover.

MILNE-THOMSON, L. M. 1968 *Theoretical Hydrodynamics*, 5th edn., chap. 13. Macmillan.

ROBINSON, A. & LAURMANN, J. A. 1956 *Wing Theory*, chap. 5. Cambridge University Press.

ROSENHEAD, L. 1931 *Proc. Roy. Soc.* A **134**, 70.

SHANKS, D. 1955 *J. Math. Phys.* **34**, 1.

SYNGE, J. L. 1926 *Proc. Roy. Irish Acad.* A **37**, 95.

WOOD, C. J. 1971 *J. Sound Vib.* **14**, 91.

WOOD, C. J. & KIRMANI, S. F. A. 1970 *J. Fluid Mech.* **41**, 627.